Cerebral Cortex, 2025, **35**, bhaf328
https://doi.org/10.1093/cercor/bhaf328
Advance access publication date 9 December 2025
Original Article

The perceptual and neural processing of familiar faces is shaped by the statistical regularities of real-world viewing

Bartholomew P.A. Quinn [1,*] and Timothy J. Andrews [2,*]

[1]Institute of Cognitive Neuroscience, University College London, Alexandra House, 17-19 Queen Square, London, WC1N 3AZ, United Kingdom
[2]Department of Psychology, University of York, Heslington, York, YO10 5DD, United Kingdom

*Corresponding authors: Bartholomew P.A. Quinn, Institute of Cognitive Neuroscience, University College London, Alexandra House, 17-19 Queen Square, London, WC1N 3AZ, United Kingdom. Email: bee.quinn@ucl.ac.uk; Timothy J. Andrews, Department of Psychology, University of York, Heslington, York, YO10 5DD, United Kingdom, Email: timothy.andrews@york.ac.uk

Face recognition depends upon the ability to match a visual image to a representation stored in memory. During natural viewing, observers fixate centrally on faces, resulting in face parts appearing in specific spatial locations. We examined whether this perceptual experience influences the cognitive and neural mechanisms involved in face recognition. Participants viewed left/right or upper/lower face halves presented in typical (eg left face half in left visual field) or atypical (eg left face half in right visual field) locations. For familiar faces, familiarity judgments were faster and more accurate when face halves were displayed in typical locations. To examine the neural correlates of this recognition bias, fMRI was used to measure responses to familiar face halves presented in typical or atypical spatial locations. Early visual areas (V1–V4) showed responses primarily determined by visual field and were not sensitive to typical spatial presentation. In contrast, the occipital face area and the fusiform face area exhibited greater activations for face halves presented in their typical spatial location. This bias was also evident in regions beyond the visual brain. These findings suggest that higher-level representations used in the perceptual processing of familiar faces are influenced by statistical regularities in real-world face viewing.

Keywords: face recognition; Ffa; Fmri; Ofa; perceptual experience.

Introduction

A growing body of evidence indicates that the visual regions involved in object recognition are not only tuned to the diagnostic features of object categories, but also to their characteristic spatial configurations (DiCarlo and Maunsell 2003; Kravitz et al. 2008; Kravitz et al. 2010). Neural responses in these regions reflect statistical regularities in the retinal positioning of objects (Levy et al. 2001; Hasson et al. 2002). This suggests that the typical spatial location of objects plays a crucial role in the functional organization of higher-level visual areas (Arcaro and Livingstone 2017; Arcaro et al. 2019; Gomez et al. 2019).

During face perception, observers—on average—fixate slightly below the eyes, near the horizontal midpoint (Hsiao and Cottrell 2008; Walker-Smith et al. 2013). This strategy optimizes recognition by positioning informative facial features within the high-acuity foveal region (Peterson and Eckstein 2012, 2013). Consequently, as shown in Fig. 1, individual facial features are systematically projected to distinct regions of the visual field, which are mapped retinotopically in the early visual cortex (Wandell et al. 2007). The upper half of the face projects to ventral visual areas (eg V1v, V2v, and V3v), while the lower half projects to dorsal visual areas (eg V1d, V2d, and V3d). Additionally, the left and right halves of the face project to contralateral hemispheres (Hsiao et al. 2008), leading to the early-stage segregation of facial information in the visual brain.

Beyond early visual areas, regions in the occipital and temporal cortices play key roles in the processing of faces (Kanwisher 2010). The occipital face area (OFA) is thought to encode the basic structural configuration of a face, before transmitting this information to the fusiform face area (FFA) to process the invariant information used in tasks such as identity recognition, and to the superior temporal sulcus (STS) to extract the variable information used in tasks such as expression recognition (Haxby et al. 2000; Duchaine and Yovel 2015). Although these regions are face-selective, they also exhibit spatial biases, responding preferentially to faces presented centrally (Levy et al. 2001; Hasson et al. 2002), or in the contralateral visual field (Silson et al. 2016; Silson et al. 2022). Emerging evidence suggests that these regions may be organized into faciotopic maps, wherein cortical responses are topographically tuned to specific facial features (Henriksson et al. 2015; de Haas et al. 2021; though see van den Hurk et al. 2015). The notion of faciotopic maps is supported by behavioral studies, showing improved discrimination of unfamiliar face parts when they appear in their typical spatial locations (Chan et al. 2010; de Haas et al. 2016; de Haas and Schwarzkopf 2018). However, whether these spatial typicality biases extend to the recognition of familiar faces remains unclear.

Received: June 23, 2025. **Revised:** October 16, 2025. **Accepted:** November 4, 2025

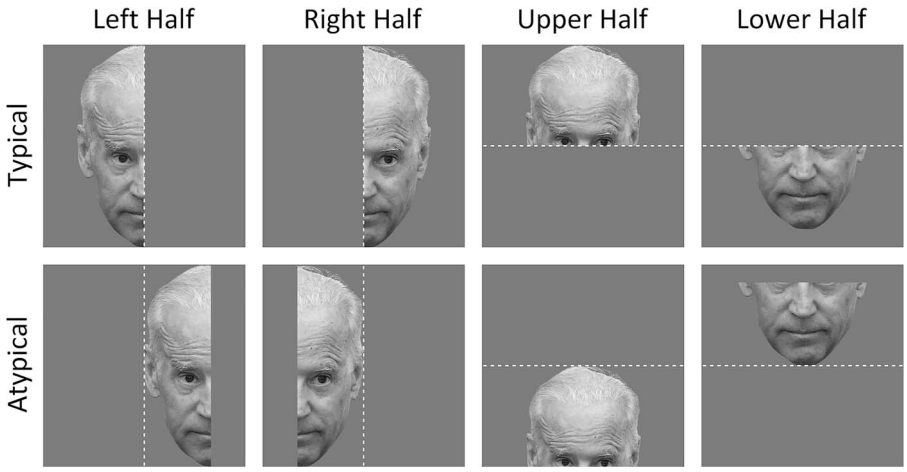

Fig. 1. Examples of typical and atypical spatial locations for face half stimuli from a famous identity (former U.S. President Joe Biden). Dotted lines are presented here for visual field division clarity, but were not present in any experiment. Images are reproduced here under a Creative Commons license. Source: https://www.flickr.com/photos/58993040@N07/13958803406, Attribution: U.S. Embassy Kyiv, Ukraine, public domain mark.

Given that experience plays a fundamental role in shaping both the behavioral and neural mechanisms underlying face processing (Golarai et al. 2015), the present study investigated how the statistical regularities of real-world viewing influence familiar face recognition. In the initial behavioral experiment, we examined whether recognition performance differs when vertically (left/right) or horizontally (upper/lower) divided face halves are presented in their typical versus atypical visual field locations. In the second experiment, we used functional magnetic resonance imaging (fMRI) to explore whether face-selective neural responses vary as a function of typical spatial positioning. Our findings demonstrate that typical spatial presentation—reflecting natural viewing habits—modulates both behavioral performance and neural activity during familiar face recognition.

Materials and methods

Behavioral experiment

Participants

Prior to data collection, sample size was determined based on power considerations and prior empirical findings. An initial benchmark was taken from Chan et al. (2010), who examined the effects of typical visual field presentation on face detection using a sample of 18 participants. A formal power analysis informed by effect sizes reported in Harrison and Strother (2020) for the perception of face halves in a comparable participant demographic indicated that a minimum of 28 participants would be sufficient to detect effects with a 2x2 within-subject ANOVA ($d = 0.60$, $\alpha = 0.05$, power = 0.95). A total of 43 participants were recruited, 11 of whom were excluded due to insufficient familiarity with the celebrity faces used (<50%), or failure to meet the laterality quotient to indicate dominant rightward handedness (<+40) as determined by a modified Edinburgh Handedness Inventory (Oldfield 1971). The remaining 32 right-handed (mean laterality quotient = 83.3, $SD = 16.7$) participants (29 female; mean age = 19.2, $SD = 0.7$) were randomly divided into 16 counterbalancing groups. All participants reported normal or corrected-to-normal vision and no known neurological disorders. They provided written informed consent and were compensated with course credit. All experiments were approved by the ethics committee of the University of York Psychology department (Approval code: 116).

Stimuli

"Familiar" face half stimuli were created from 40 front-facing high-resolution images of famous people (ie actors, politicians, and musicians), collected using Google image search. "Unfamiliar" face half stimuli were created from 40 front-facing, high-resolution face images of non famous individuals, collected from different face database repositories (SiblingsDB, Vieira et al. 2014; Chicago Face Database, Ma et al. 2021; The London Set, DeBruine and Jones 2017) and stock photo repositories (www.unsplash.com, and www.gettyimages.co.uk). Unfamiliar face images were individually selected based on comparability to one of the familiar face identities (similar hair color/style, skin tone, & face shape). All 80 faces were standardized by cropping them from backgrounds, converting them to greyscale, and pasting them onto a uniform gray background. Faces were then halved vertically (left and right halves) at the midpoint of the nose, and horizontally (upper and lower halves) slightly below the eyes. Vertically divided halves were resized to a height of 500 px, and horizontally divided halves were resized to a width of 350 px.

Procedure

The experiment was conducted in-person. Participants were seated in an evenly lit laboratory with their chin in a chinrest that was 80 cm away from the computer screen (width = 54 cm; height = 30 cm). At this distance, face halves subtended a height of approximately 9.2° of visual angle for vertically divided face halves, and 6.5° of visual angle for horizontally divided face halves. The experiment was built using PsychoPy (Version 2021 February 3; www.psychopy.org) and consisted of three blocks.

First, participants viewed vertically or horizontally divided face halves in separate blocks. The ordering of the blocks was counterbalanced across participants. Each of these two blocks began with a series of practice trials, in which participants viewed five familiar and five unfamiliar face halves in either typical or atypical spatial locations. The identities of these faces were not used elsewhere in the experiment and were used solely to familiarize participants with the block's task. In each block, participants viewed the two face halves from each identity (40 familiar and 40 unfamiliar). Each face half was presented in its typical spatial location (eg right half in right visual field) or in its atypical spatial location (eg left half in right visual field). This generated a total of 160 trials in each block. Within the experiment, there were an even

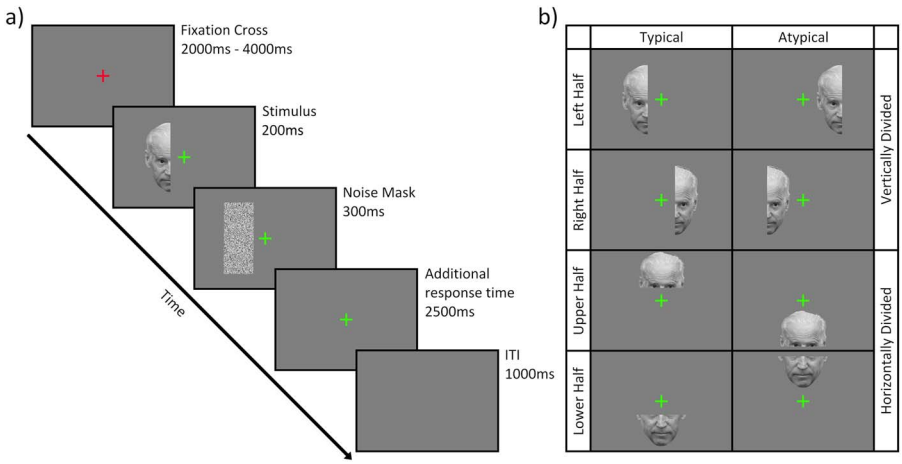

Fig. 2. Schematic of behavioral experiment trials for a single familiar identity (former U.S. President Joe Biden): a) vertically divided, left half, typical presentation trial. b) Grid of example presentations arranged into rows displaying face half and division conditions, and columns displaying spatial location typicality.

number of trials for each visual field presentation and typicality condition. Which face halves appeared in which spatial locations were evenly counterbalanced across participants.

As illustrated in Fig. 2, trials began with a red fixation cross, which appeared in the centre of the screen for a random interval between 2000 ms and 4000 ms. The cross then turned green, and simultaneously, a face half appeared in either a typical or atypical visual field, with its nearest side positioned 2.75° of visual angle away from the fixation cross to avoid bilateral visual field presentation (Bourne 2006; Young 1982). Face halves were presented for 200 ms, before being replaced by a Gaussian noise mask to avoid foveal saccades towards the stimulus (Carpenter 1988; Bourne 2006). The mask vanished after 300 ms. Throughout the presentation of the face half and mask, the green fixation cross stayed centrally on screen, and remained on screen for a further 2500 ms. The fixation cross then disappeared for an inter-trial-interval of 1000 ms before the next trial began.

Participants were asked to indicate whether the face half that had been presented was familiar or unfamiliar by pressing a key. Participants had the duration of the green fixation cross (3000 ms) to input their responses on a keypad. For vertically divided face halves, participants were instructed to respond using the "up arrow" and "down arrow" keys; for horizontally divided face halves participants were instructed to respond using the "left arrow" and "right arrow" keys. Response hand (left or right hand) and response input key (eg up equals familiar and down equals unfamiliar; or down equals familiar and up equals unfamiliar) were counterbalanced across participants. Accuracy and reaction time for correct responses were recorded.

In the final block, we determined whether participants were familiar or unfamiliar, respectively, with the identities used in the previous blocks. Full versions of all 80 faces were presented centrally on screen, and participants indicated whether they recognized a face by inputting a name, or relevant identity-specific information into a textbox (eg a specific role they had played in a film). If participants did not recognize the individual, they could respond with a button press and move to the next trial. Any trials featuring face halves from faces which were incorrectly identified were excluded from the analysis of the initial two blocks. Any participants who were unable to identify over 50% of the familiar identities used were completely removed from the analyzed sample.

The study design, hypotheses, and analysis plan for this experiment were preregistered (https://osf.io/4t9rv). Data and analysis code for this and the subsequent experiment is publicly available on the Open Science Framework website (https://osf.io/dbufh). Our preregistered hypotheses test the following predictions: H1) If recognition is affected by typicality of spatial location presentation, then recognition will be improved and more efficient for face halves within their typically experienced visual fields across both vertically and horizontally divided face halves; H2). If the typicality of spatial location presentation is relevant to the matching of familiar face representations in memory, then we should see enhanced effects of typicality for familiar faces. Familiar and unfamiliar faces are not made publicly available for copyright reasons, but examples are provided in this paper.

Neuroimaging experiment

Participants

Prior to data collection, sample size was based on a minimum determined by an fMRI study by Chan et al. (2010). For the sample to be scanned, we recruited a separate sample of participants who had not taken part in the behavioral study. 33 participants were screened to ensure applicability for fMRI scanning and right-handedness (<+40 laterality quotient; Oldfield 1971). During screening, participants completed the final block described in the behavioral experiment to assess their familiarity with the celebrity faces to be used during scanning. Any participants who recognized <80% of the identities were excluded. 13 participants did not pass the screening. The remaining 20 participants (mean laterality quotient = 64.7, *SD* = 25.0; 17 female; mean age = 20.9, *SD* = 1.9; mean identities known = 93.6%) were randomly divided into four counterbalancing groups. All participants reported normal or corrected-to-normal vision, and no known neurological disorders. They provided written informed consent and were compensated with course credit. All experiments were approved by the ethics committee of the University of York Neuroimaging Centre (Approval code: P1491).

Stimuli

Participants completed two experimental scan runs; one contained vertically divided face halves, and the other contained horizontally divided face halves. The ordering of scan runs was counterbalanced across participants. Stimuli within each run

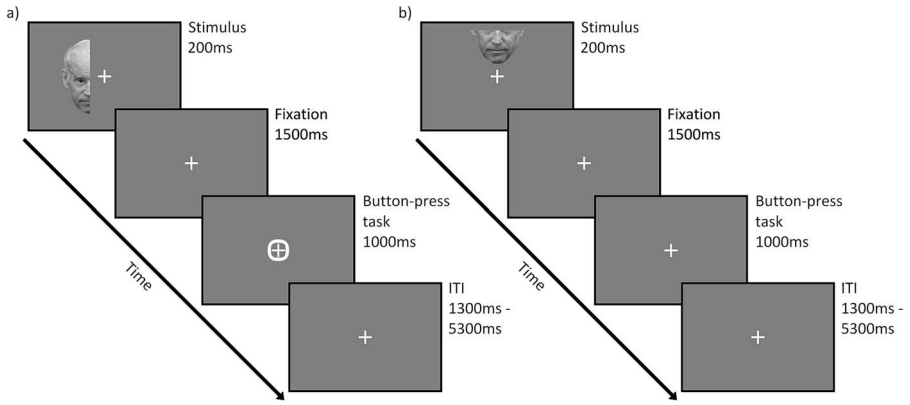

Fig. 3. Example schematics of fMRI experiment trials for a single familiar identity (former U.S. President Joe Biden): a) vertically divided, left half, typical presentation trial with button press circle. b) Horizontally divided, upper half, atypical presentation trial with no button press circle. Possible stimulus presentations are depicted in Fig. 2b.

were the face half stimuli from the same 40 familiar identities used in the behavioral experiment. Participants viewed the faces from a distance of 62 cm. To match our behavioral experiment conditions, the stimuli were shown at a height of 9.2° of visual angle for vertically divided face halves, and 6.5° of visual angle for horizontally divided face halves.

As illustrated in Fig. 3, throughout each task run, a white fixation cross remained in the centre of the screen. 80 images (two face halves from each identity) were presented in each run using an event-related design, featuring 40 stimuli for each face half (left/right or up/down), and spatial location (typical or atypical) condition. Face halves appeared in either their typical or atypical spatial locations, with their nearest side positioned 2.75° of visual angle away from the fixation cross. All participants saw the same set of stimuli. Each image was presented for 200 ms, with a jittered presentation of 3800–7800 ms between each image for a total scan time of 440 s. Event-related design sequencing was performed using OptSeq2 (https://surfer.nmr.mgh.harvard.edu/optseq) to generate the two most optimal sequences out of 10,000, which were evenly counterbalanced across participants.

In contrast to the behavioral experiment, participants did not make a familiarity judgment, as the face identities were all "familiar". However, to maintain attention, participants were instructed to execute a button-press whenever they saw a white circle around the fixation cross. This cross appeared on 10% of trials, 1,500 ms after stimulus presentation, and remained on screen for a further 1,000 ms.

Participants also completed a functional localiser scan run. During this scan, participants viewed images drawn from three different stimulus categories (human faces, scenes, and phase-scrambled images). Face stimuli were taken from the Radboud database of face stimuli (Langner et al. 2010), scene stimuli were taken from the SUN database (Xiao et al. 2010), and scrambled images were created by phase-scrambling the face stimuli. Images from each condition were presented in a block design. 12 images were presented in each block, and each image was presented for 600 ms, with a 200 ms inter-trials-interval. Nine blocks were presented for each condition in a pseudorandomised order, for a total scan time of 244 s. To ensure that attention was maintained on the stimuli, the same fixation cross and task as featured in the task runs were repeated here.

fMRI acquisition and analysis

Structural and functional scans were acquired at the York Neuroimaging Centre using a whole-body 3 Tesla Siemens MAGNETOM Prisma MRI scanner during the same session, using a 64-channel phased array head coil. T1-weighted structural scans, composed of 176 sagittal slices, were acquired from gradient-echo echo-planar imaging pulse sequences (TR = 2300 ms, TE = 2.26 ms, FoV = 240 × 240 mm, matrix size = 256 × 256, voxel dimensions = 1.0 × 1.0 × 1.0 mm, slice thickness = 1.0 mm, flip angle = 8°, whole-brain coverage).

Task and functional localiser scans, composed of 60 axial slices, were acquired from T2∗-weighted gradient-echo echo-planar imaging pulse sequences (TR = 2,000 ms, TE = 30 ms, FoV = 240 × 240 mm, matrix size = 80 × 80, voxel dimensions = 3.0 × 3.0 × 3.0 mm, slice thickness = 3.0 mm, flip angle = 80°, whole-brain coverage, phase encoding direction anterior to posterior). Additional field-map images were acquired in the same plane as the functional images (TR = 554 ms, TE = 7.38 ms, flip angle = 60°, other parameters as per functional images).

A univariate analysis of the data was conducted using FSL FEAT v.6.00 (https://fsl.fmrib.ox.ac.uk). First-level analysis of the experimental and functional localiser scans was conducted on each participant individually. These included motion correction using MCFLIRT (https://fsl.fmrib.ox.ac.uk; Jenkinson et al. 2002), slice timing correction using Fourier-space time-series phase shifting, nonbrain removal using BET (Smith 2002), unwarping of B0 distortions from fieldmaps, intensity normalization, temporal high-pass filtering (task, σ = 100.0 s; localiser σ = 50.0 s), and spatial smoothing (Gaussian) at 6 mm (full width at half maximum).

For each run of the experimental scans, the BOLD response was modeled using a separate explanatory variable for each of the four stimulus types, defined as a Face Half (left/right or up/down) + Typicality (typical presentation/atypical presentation). The presentation design was convolved with a gamma haemodynamic response function to produce an anticipated BOLD response. The temporal derivative of this time course was included in the model for each exploratory variable, and data were fitted to FSL's implementation of the general linear model. For the functional localiser data, boxcar regressors were defined for each task condition (faces, scenes, and phase-scrambled faces), and convolved with a gamma haemodynamic response function. Individual participant data was then entered into a higher-level group analysis using a mixed-effects design in FLAME (FLAME, https://fsl.fmrib.ox.ac.uk; Beckmann et al. 2003; Woolrich et al. 2004; Woolrich 2008). Functional images were co-registered to each participant's T1 anatomical scan via a boundary-based registration algorithm (Greve and Fischl 2009), and then further to the standard MNI

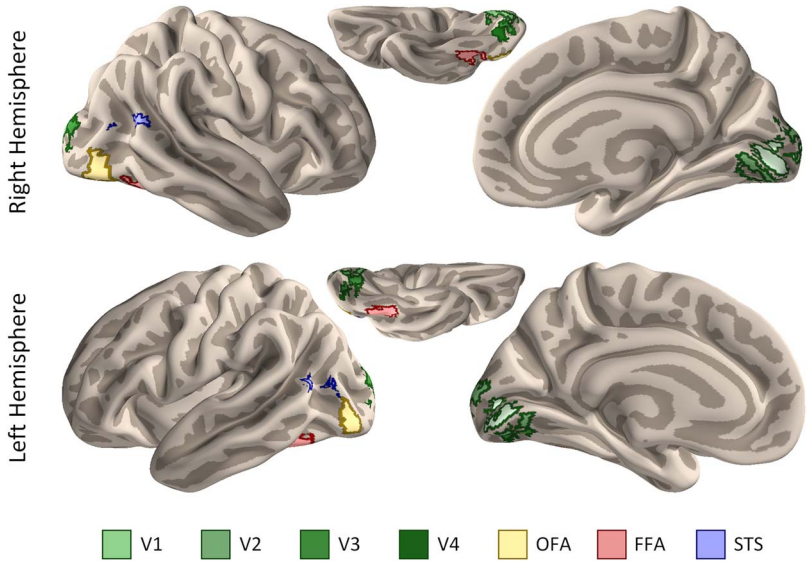

Fig. 4. Regions of interest. Face regions were defined using the functional localiser scans (OFA, occipital face area; FFA, fusiform face area; STS, superior temporal sulcus). Early visual regions (V1, V2, V3, and V4) were based on visual field masks (Wang et al. 2015).

brain (ICBM152) via FSL's FNIRT tool (Andersson and Skare 2010).

The localiser scan revealed the face-selective regions of interest (ROIs) shown in Fig. 4. These included the OFA, FFA, and posterior STS. For our primary analysis, ROIs were defined based on the functional localiser group averages, rather than each individual participant. The rationale for doing so was to maintain a consistent voxel count across participants, as consistently sized clusters were not attainable for all participants, particularly for face-selective ROIs in the left hemisphere. Seed points for each ROI within each hemisphere, listed in Table S3, were defined as the peak activation voxel for the face>other (scenes + scrambled faces) contrast. For each seed, a flood fill algorithm was used to iteratively adjust the statistical threshold to identify clusters of 200 contiguous voxels (2,000 mm^3) around the seed. This process was repeated for each seed to create masks for each ROI.

For a secondary analysis, face-selective ROIs were also defined for each participant using the same clustering methodology. These proved less consistent than those derived from the group localiser. To compensate for this, the individual participant ROI size was reduced to 150 contiguous voxels (1500 mm^3). All ROIs which could be identified at approximately this volume from individual participant localisers were included in the analysis; any ROI clusters which could not be defined from this criterion were excluded from analysis. The number of participants in whom ROIs could be successfully defined ranged from 12 to 14 ($M = 13.3$, $SD = 0.82$). Individual participant seed points for each ROI are defined in Table S4, and their ROI sizes and z-thresholds are listed in Table S5.

In addition to these face-selective ROIs, we also defined ROI masks for early visual areas within each hemisphere (V1d, V2d, V3d, V1v, V2v, V3v, and V4) based upon visual field masks generated by Wang et al. (2015). For each mask, 200 voxel clusters were created from the full probability maps provided by Wang et al. (2015). Seed points for each ROI, listed in Table S3, were defined as the peak probability of being a given early visual area, and the same flood fill algorithm was used to identify clusters of high-probability spatially contiguous voxels around the seed, restricted within their respective Wang et al. (2015) masks. To compare left and right visual field effects, the dorsal and ventral divisions of each early visual region were combined into a single mask for each hemisphere (rV1, lV1, rV2, lV2, rV3, lV3, rV4, and lV4). To compare upper and lower visual field effects, the ventral and dorsal regions of each early visual region were combined into separate masks (V1v, V1d, V2v, V2d, V3v, V3d, and V4), and masks from both hemispheres were combined.

FSL's Featquery was used to extract the mean hemodynamic activity in response to Visual Field (right/up, left/down) and Typicality (typical spatial location, atypical spatial location) conditions, averaged over voxels within each ROI (parameter estimate β). Potential overlaps in signal intensity from the event-related design could lead to atypical scaling of signal percentage changes. Therefore, the raw β values were used for analysis. To account for multiple comparison corrections, Holm-Bonferroni corrections were applied to t-tests for regions $*$ hemispheres within each network (early visual, face) independently for each experimental comparison.

Results

Behavioral experiment

Familiar and unfamiliar faces

We compared accuracy and accurate reaction times on familiarity judgments for face halves presented within typical or atypical spatial locations. For familiar faces, familiarity judgments for face halves presented in typical spatial locations were more accurate and faster compared to face halves presented in atypical spatial locations. In contrast, there was no effect of typical spatial location on familiarity judgments for unfamiliar faces.

A repeated-measures ANOVA on the effects of Familiarity (familiar, unfamiliar), Typicality (typical spatial location, atypical spatial location), and Division (vertical, horizontal) is reported in full in Table S1. There was a main effect of Typicality on accuracy [$F(1, 31) = 40.19$, $P < 0.001$, $\eta_p^2 = 0.56$] and reaction time [$F(1, 31) = 7.49$, $P = 0.010$, $\eta_p^2 = 0.20$]. There was also a significant interaction between Familiarity and Typicality [accuracy: $F(1, 31) = 37.54$, $P < 0.001$, $\eta_p^2 = 0.55$; reaction time: $F(1, 31) = 10.72$, $P = 0.003$, $\eta_p^2 = 0.26$]. Accordingly, we analyzed the effect of

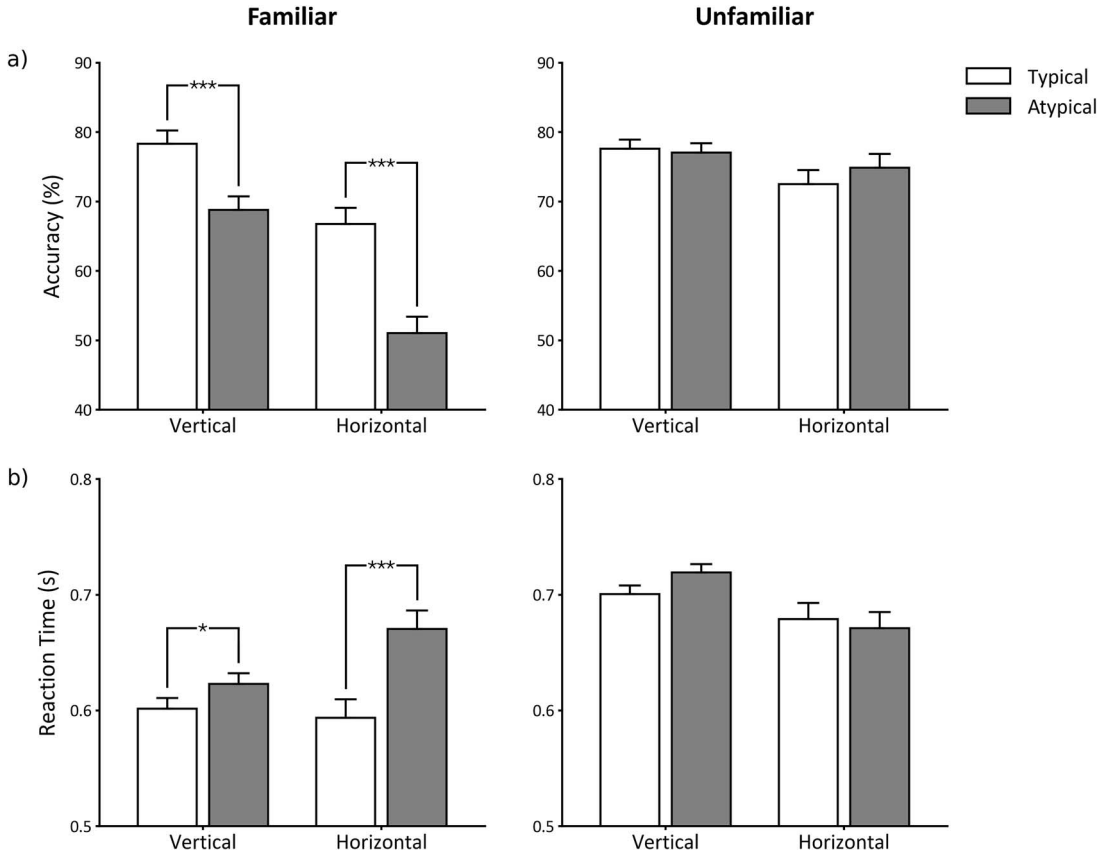

Fig. 5. There were a) higher accuracy and b) lower reaction times for familiar faces viewed in typical compared to atypical spatial locations. This effect was evident for faces divided along both the vertical and horizontal axes. There were no effects of typicality for unfamiliar faces.

Typicality on familiar faces and unfamiliar faces independently. The results of this analysis are shown in Fig. 5, and descriptive statistics are provided in Table S2.

Familiar faces

Repeated-measures ANOVAs were used to assess the effect of Typicality (typical spatial location, atypical spatial location) and Division (vertical, horizontal) on the accuracy and accurate reaction times to familiar faces.

For accuracy (Fig. 5a), there was a significant effect of Typicality [$F(1, 31) = 56.90$, $P < 0.001$, $\eta_p^2 = 0.65$], a significant effect of Division [$F(1, 31) = 33.52$, $P < 0.001$, $\eta_p^2 = 0.52$], and an interaction [$F(1, 31) = 4.82$, $P = 0.036$, $\eta_p^2 = 0.14$]. Holm–Bonferroni corrected paired sample *t*-tests on the effects of Typicality on each Division direction showed that vertically divided face halves were recognized more accurately when presented in their typical spatial locations than when presented in atypical spatial locations [$t(31) = 4.81$, $P < 0.001$, $d = 0.62$]. A greater magnitude advantage for typical presentation was also evident in horizontally divided face halves [$t(31) = 6.60$, $P < 0.001$, $d = 1.09$].

For reaction time of correct judgments (Fig. 5b), there was a significant effect of Typicality [$F(1, 31) = 24.48$, $P < 0.001$, $\eta_p^2 = 0.44$], no effect of Division [$F(1, 31) = 1.06$, $P = 0.310$], and a significant interaction [$F(1, 31) = 9.79$, $P = 0.004$, $\eta_p^2 = 0.24$]. Holm-Bonferroni corrected paired sample *t*-tests showed that face halves were recognized faster when presented in their typical spatial locations across both vertically [$t(31) = 2.27$, $P = 0.030$, $d = 0.20$] and horizontally [$t(31) = 4.72$, $P < 0.001$, $d = 0.65$] divided face halves.

Unfamiliar faces

The same ANOVA used for familiar faces was repeated for accuracy and accurate reaction times to unfamiliar faces.

For accuracy (Fig. 5a), there were no significant effects of Typicality [$F(1, 31) = 0.72$, $P = 0.402$], Division [$F(1, 31) = 1.41$, $P = 0.244$], nor any interaction [$F(1, 31) = 1.41$, $P = 0.306$]. For reaction time of accurate judgments (Fig. 5b), there were also no significant effects Typicality [$F(1, 31) = 0.42$, $P = 0.522$], Division [$F(1, 31) = 2.96$, $P = 0.095$], nor any interaction [$F(1, 31) = 2.85$, $P = 0.101$].

Neuroimaging experiment

Visual field effects

We first compared the response to stimuli presented in the left and right visual field (see Fig. 2b). We predicted that early visual regions within each hemisphere would respond selectively to stimuli presented in the contralateral visual field. Figure 6 shows the response to faces presented in the left or right visual field. Face halves presented in the left visual field resulted in higher activity in the right hemisphere compared to face halves presented in the left visual field. In contrast, face halves presented in the right visual field resulted in higher activity in the left hemisphere compared to face halves presented in the left visual field. These effects were primarily evident in the occipital lobe.

To determine which regions showed an effect, we performed an ROI analysis. Paired-sample *t*-tests were used to assess the effect of Visual Field (Right, Left) on the magnitude of activation (Parameter Estimate β) on the ROIs independently for each hemisphere. Results are listed in Table 1, and descriptive statistics are provided in Table S6. There was a significant effect of Visual Field in all early

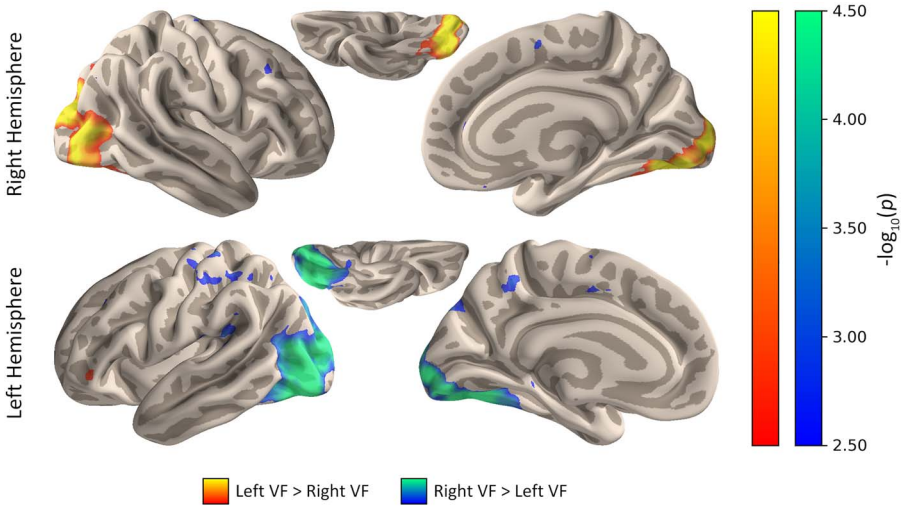

Fig. 6. Differences in neural response to faces presented in the left and right visual field. Vertically divided face halves presented to the left or right visual field elicited activation in the contralateral hemisphere. *P*-values are represented in negative log units ($-\log_{10}(p)$).

Table 1. A comparison of contralateral vs ipsilateral visual field presentation on the neural response in early visual and face-selective regions in the left and right hemispheres.

	df	t	P	d_{avg}	BF_{10}
Right Hemisphere					
V1	19	−4.38	<**0.001**	1.04	98.16
V2	19	−8.85	<**0.001**	1.78	>1000
V3	19	−11.85	<**0.001**	1.89	>1000
V4	19	−8.9	<**0.001**	1.44	>1000
OFA	19	−4.74	<**0.001**	0.77	204.02
FFA	19	−2.04	0.056	0.39	1.27
STS	19	−0.77	0.453	0.17	0.30
Left Hemisphere					
V1	19	4.57	**0.001**	0.91	>1000
V2	19	5.7	<**0.001**	1.43	>1000
V3	19	8.67	<**0.001**	1.88	>1000
V4	19	8.42	<**0.001**	1.75	>1000
OFA	19	9.29	<**0.001**	1.69	>1000
FFA	19	2.58	**0.018**	0.51	3.11
STS	19	4.52	**0.001**	1.05	129.80

visual regions (V1–V4), with a greater response to presentations in the contralateral hemisphere. The effect of Visual Field was also evident bilaterally in the OFA, but was only found to be significant in the FFA and STS of the left hemisphere.

The same analysis was conducted on individually defined face-selective ROIs, the results of which are listed in Table S7. This showed a comparable pattern, with significant effects of Visual Field in the OFA, FFA, and STS within the left hemisphere. As in the main analysis, the OFA was the only face-selective region to show an effect of Visual Field in the right hemisphere.

Next, we compared the response to stimuli presented in the upper and lower visual field (see Fig. 2b). We predicted that ventral and dorsal early visual regions within each hemisphere would respond preferentially to stimuli presented to the upper and lower visual field, respectively. Figure 7 shows the response to faces presented in the upper and lower visual field. Face halves presented in the upper visual field resulted in higher activity in ventral regions compared to face halves presented in the lower visual field. In contrast, face halves presented in the lower visual field resulted in higher activity in dorsal regions compared to face halves presented in the upper visual field. These effects were primarily evident in the occipital lobe.

To determine which regions showed an effect, we performed an ROI analysis using the early visual region and face-selective region masks. Paired-sample *t*-tests were used to assess the effect of Visual Field (Up, Down) on the magnitude of activation (Parameter Estimate β) on the ROIs from both hemispheres combined. Results are listed in Table 2, and descriptive statistics are provided in Table S6. There was a significant effect of Visual Field presentation in all the early visual regions, with a greater response to the upper visual field in V1v-V3v and a greater response to the lower visual field in V1d–V3d. There was also a significantly greater response to the upper visual field in V4 and the lower visual field in the OFA.

The same analysis was conducted on individually defined face-selective ROIs, the results of which are listed in Table S7. This showed no significant bias for Visual Field across all regions.

Typicality effects

To identify the effects of typicality, we compared the responses to stimuli presented in typical versus atypical spatial locations (see

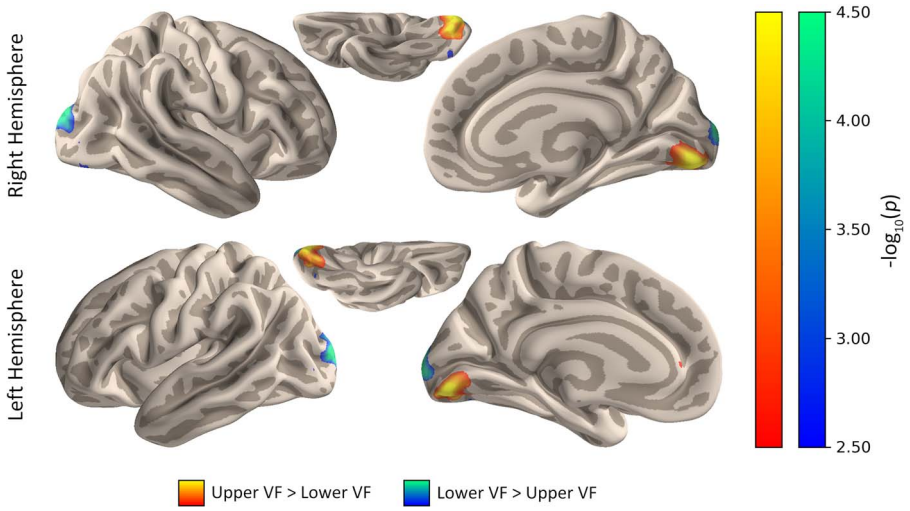

Fig. 7. Differences in response to faces presented in the upper and lower visual fields. Horizontally divided face halves presented to either the upper or lower visual field elicited differences in response in dorsal and ventral regions of early visual cortex. P-values are represented in negative log units ($-\log_{10}(p)$).

Table 2. A comparison of upper vs lower visual field presentation on the neural response in early visual and face-selective regions combined across hemispheres.

	df	t	*P*	d_{avg}	BF_{10}
Combined Hemispheres					
V1v	19	4.24	<**0.001**	0.83	74.15
V2v	19	4.27	<**0.001**	1.14	79.53
V3v	19	5.45	<**0.001**	1.22	826.52
V1d	19	−2.94	**0.008**	0.60	5.94
V2d	19	−7.62	<**0.001**	1.80	>1000
V3d	19	−7.70	<**0.001**	1.53	>1000
V4	19	3.53	**0.002**	0.80	18.23
OFA	19	−2.67	**0.015**	0.31	3.66
FFA	19	−0.45	0.661	0.07	0.25
STS	19	−0.01	0.994	0.00	0.23

Fig. 2b). If typical spatial location presentation is important for recognition, we expected a greater magnitude of response to face halves presented in their typical spatial locations. This analysis was performed separately for vertically and horizontally divided faces. Figure 8 shows regions that showed higher responses to face halves in the typical spatial location. This effect was evident in the visual brain, but was also evident in the regions beyond the visual brain. Table 3 shows the location of all clusters exceeding 500 mm^3 which showed significant typicality effects ($P > 0.05$). Whole brain analysis was also performed for atypical>typical contrasts, and results are shown in Fig. S1 & Table S8.

An ROI analysis was performed to explore the effect of face halves presented in their typical spatial locations. Figure 9 shows the effect of Typicality in the face regions. Paired-sample *t*-tests were used to assess the effect of Typicality on the magnitude of response in all ROIs. Results are listed in Table 4, and descriptive statistics are provided in Table S9. As shown in Fig. 9, There was a higher magnitude of response in the OFA to faces presented in typical spatial locations. This was also evident for the FFA, but only for horizontally divided face halves. However, there was no effect of Typicality in the STS or in early visual areas. To retain consistency with the visual field analysis, Typicality results for horizontally divided face halves were also calculated for ROIs combined across hemispheres. Results and descriptive statistics for this analysis are provided in Table S10. This showed much the same pattern as in divided hemispheres, with higher magnitude responses to faces presented in typical spatial locations in the OFA and FFA, but in no other examined regions.

Finally, a corresponding analysis was conducted on individually defined face selective ROIs. Results and descriptive statistics for this analysis are provided in Table S11 (vertically divided faces) & Table S12 (horizontally divided faces). Consistent with the main analyses, this showed higher magnitude responses to faces presented in typical spatial locations for the OFA across all conditions and hemispheres, while the STS did not show any effects of Typicality. Similar to the main analysis, the FFA only showed a typicality bias in response to horizontally divided faces. This was significant in the right FFA, but not the left FFA—which only trended in this same direction, potentially reflecting the reduced power of the individually defined ROI sample.

Discussion

This study investigated whether the spatial patterns of natural face viewing shape the cognitive and neural mechanisms underlying familiar face recognition. Our findings show that (1) familiar faces are recognized more accurately and efficiently when presented in their typical spatial locations, and (2) face-selective

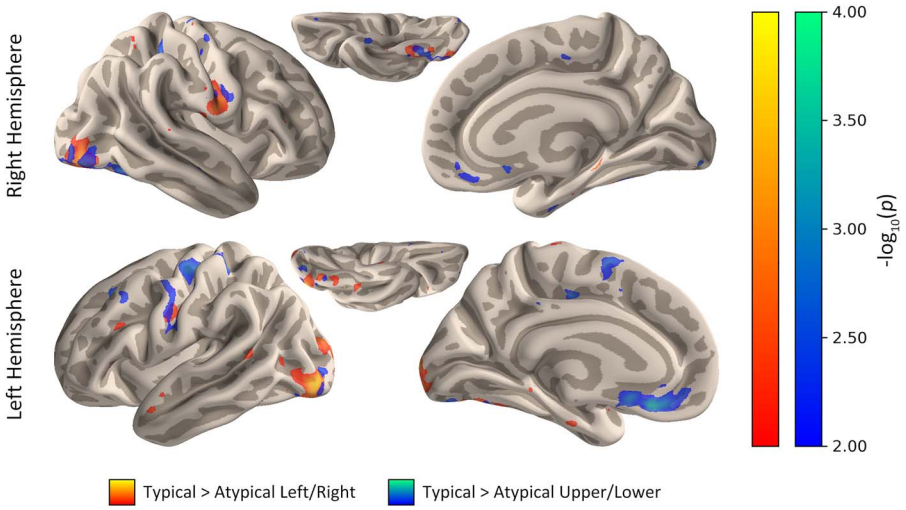

Fig. 8. Differences in the response to faces presented in typical compared to atypical spatial locations for left and right face halves and upper and lower face halves. The effect of typicality is evident in the core face regions, but also in regions beyond the visual brain. P-values are represented in negative log units ($-\log_{10}(p)$).

Table 3. Peak MNI coordinates of > 500 mm^3 clusters showing greater responses for typical vs atypical presentations of faces.

	hemi	x	y	z	Cluster Size (mm^3)	Threshold *Z*
Vertical						
Lateral Occipital Cortex (inferior)	L	−40	−86	−6	7280	3.50
Occipital Pole	L	−8	−102	8	5160	3.67
Lateral Occipital Cortex (inferior)	R	46	−80	−10	3880	3.48
Postcentral Gyrus	R	58	−8	18	2480	3.13
Precentral Gyrus	L	−52	−8	32	1800	3.05
Occipital Fusiform Gyrus	R	38	−64	−18	1090	2.61
Lingual Gyrus	L	−12	−60	−10	940	3.30
Occipital Fusiform Gyrus	L	−35	−66	−10	610	2.77
Hippocampus	R	24	−30	−8	510	3.17
Horizontal						
Postcentral Gyrus	L	−30	−30	54	3610	3.26
Subcallosal Cortex	L	−8	30	−14	3120	3.43
Precentral Gyrus	L	−54	−12	44	2410	2.96
Lateral Occipital Cortex (inferior)	R	46	−76	−12	1770	2.94
Occipital Pole	R	6	−94	−8	1390	3.18
Postcentral Gyrus	R	28	−34	48	1270	3.21
Lingual Gyrus	L	−12	−88	−12	1170	3.07
Lateral Occipital Cortex (inferior)	L	−37	−88	−10	970	2.57
Temporal Occipital Fusiform Cortex	R	40	−54	−16	960	2.85
Precentral Gyrus	L	46	−8	26	930	2.80
Occipital Fusiform Gyrus	L	36	−74	10	770	2.90
Juxtapositional Lobule Cortex	L	−2	8	64	690	2.87
Middle Frontal Gyrus	R	34	14	52	640	2.84
Superior Frontal Gyrus	L	−20	26	42	620	3.01

regions in the brain showed enhanced responses to familiar faces viewed in typical spatial locations. Together, these findings are consistent with the idea that typicality enhances representational efficiency in higher-level visual cortex (Iordan et al. 2016).

During natural viewing, fixations tend to be centrally positioned on faces, resulting in consistent visual field mappings of facial features (Hsiao and Cottrell 2008; Walker-Smith et al. 2013). The left and right halves of the face are typically viewed in their corresponding visual hemifields, and the upper and lower halves likewise appear in their respective visual hemifields. Our behavioral results demonstrate that presenting faces in their typical spatial location facilitates the perception of familiarity in familiar faces, but not unfamiliar faces. Prior research has shown that perceptual matching of unfamiliar faces is enhanced when features are presented in typical spatial locations (Chan et al. 2010; de Haas et al. 2016; de Haas and Schwarzkopf 2018). The absence of a spatial typicality effect for unfamiliar faces in our behavioral experiment suggests that the advantage observed for the recognition of familiar faces is unlikely to be based purely on these lower-level perceptual biases, but extends to the matching of a perceived face to an internalized representation.

To identify the neural correlates of these spatial typicality effects, we compared responses to familiar face halves presented

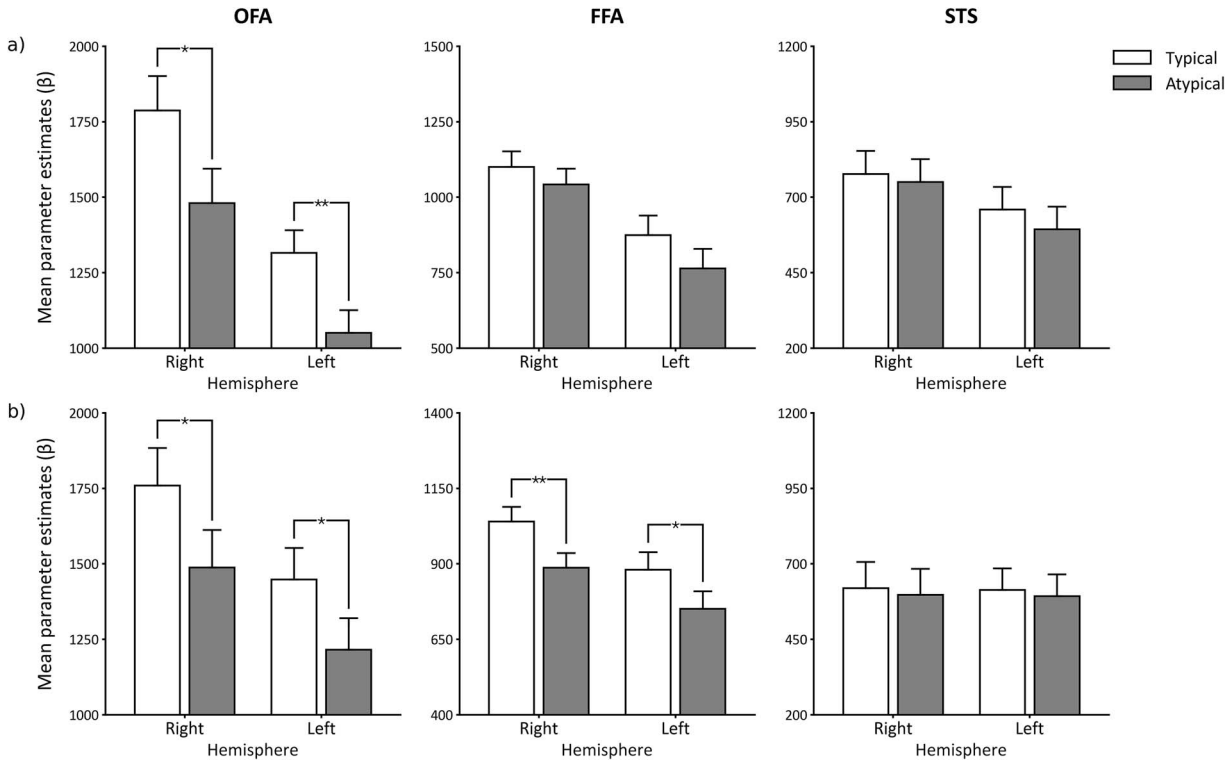

Fig. 9. The responses to familiar faces viewed in typical compared to atypical spatial locations. An effect of typicality was evident for (a) vertically divided faces in the OFA and for (b) horizontally divided faces in the OFA and FFA.

in typical versus atypical locations. Consistent with prior research (Wandell et al. 2007; Hsiao et al. 2008), early visual areas exhibited topographically organized responses based on visual field positioning. This division of contralateral or ventral/dorsal selectivity in early visual regions indicates that the paradigm was successful in presenting facial information to the intended visual field. Visual field biases were also evident within regions of the face-selective network, particularly within the OFA, and at lower magnitudes in subsequent regions (Silson et al. 2016, 2022; de Haas et al. 2021). Despite the continuity of visual field effects across the visual brain, early visual regions did not exhibit sensitivity to spatial typicality, indicating that this effect emerges at later stages of processing.

An effect of typical spatial location was observed in face-selective regions, including the OFA and FFA. Previous studies have demonstrated distinct multivoxel activation patterns in these regions for typical versus atypical facial and featural arrangements (Chan et al. 2010; Henriksson et al. 2015; de Haas et al. 2016). However, our findings provide the first evidence of an overall increase in neural response to faces presented in the typical spatial location. The absence of an effect in earlier studies may reflect their use of unfamiliar faces, whereas the current study employed familiar faces. This explanation is supported by our behavioral findings, wherein familiar face halves were recognized more efficiently when presented in typical rather than atypical spatial locations, with no corresponding effect for unfamiliar faces. It should be noted, however, that presenting faces in atypical locations necessarily alters the polar angle and eccentricity of individual features, and eccentricity biases in face-selective regions may have contributed to the observed differences (van den Hurk et al. 2015; Morsi et al. 2024). Future research should disentangle these factors by directly comparing familiar and unfamiliar faces, to clarify whether the modulation of neural response is driven by familiarity or the visual field position of facial features.

The neural response in the OFA mirrored the behavioral bias for faces presented in typical visual fields. This suggests that this region plays a key role in familiar face recognition, extending beyond its traditionally proposed function in the detection and structural encoding of faces (Haxby et al. 2000). This interpretation aligns with lesion and deactivation studies demonstrating the OFA's critical involvement in familiar face recognition (Jonas et al. 2012; Ambrus, Dotzer, et al. 2017a; Ambrus, Windel, et al. 2017b; Ambrus et al. 2019; Eick et al. 2021). Alongside such evidence, our findings correspond with contemporary models which propose direct connections between the OFA and regions within the extended network associated with higher-level recognition, such as the anterior temporal lobe (Collins and Olson 2014; Duchaine and Yovel 2015).

The FFA showed spatial typicality effects primarily for horizontally divided faces. This fits with our behavioral findings, in which horizontally divided faces showed stronger typicality effects. The greater effect of spatial position for horizontally divided faces presumably reflects the fact that atypical spatial presentations result in a more marked disruption to the way we naturally view faces. This is similar to the well-established detrimental impact of face inversion, in which the bottom half of the face appears in the upper visual field and the lower half of the face appears in the upper visual field (Valentine 1988). In contrast, the symmetrical structure of faces along the vertical axis preserves these feature relationships, rendering recognition less sensitive to atypical spatial presentations.

No spatial typicality effects were observed in STS. This finding aligns with the role of the STS in processing dynamic facial cues that are important for social communication (Haxby et al. 2000; Harris et al. 2014; Pitcher and Ungerleider 2021).

Table 4. The effect of typical vs atypical presentations of faces on the neural response in early visual and face-selective regions.

Vertical	***df***	**t**	**P**	d_{avg}	BF_{10}
Right Hemisphere					
V1	19	0.28	0.779	0.06	0.24
V2	19	1.48	0.156	0.36	0.59
V3	19	1.33	0.199	0.25	0.50
V4	19	0.48	0.636	0.08	0.26
OFA	19	2.62	**0.017**	0.39	3.35
FFA	19	1.10	0.286	0.17	0.40
STS	19	0.35	0.733	0.05	0.25
Left Hemisphere					
V1	19	1.53	0.142	0.29	0.63
V2	19	1.62	0.121	0.41	0.71
V3	19	1.45	0.164	0.30	0.57
V4	19	1.84	0.082	0.33	0.95
OFA	19	3.45	**0.003**	0.53	15.67
FFA	19	1.67	0.110	0.31	0.76
STS	19	0.86	0.403	0.14	0.32
Horizontal	***df***	**t**	***p***	d_{avg}	BF_{10}
Right Hemisphere					
V1	19	−0.23	0.820	0.05	0.24
V2	19	−0.01	0.993	0.00	0.23
V3	19	0.56	0.581	0.10	0.27
V4	19	1.25	0.228	0.19	0.46
OFA	19	2.14	**0.046**	0.33	1.49
FFA	19	3.10	**0.006**	0.38	7.98
STS	19	0.26	0.800	0.04	0.24
Left Hemisphere					
V1	19	−0.43	0.671	0.09	0.25
V2	19	−0.32	0.752	0.07	0.24
V3	19	0.23	0.822	0.03	0.24
V4	19	1.13	0.273	0.19	0.41
OFA	19	2.17	**0.043**	0.36	1.58
FFA	19	2.20	**0.040**	0.28	1.65
STS	19	0.28	0.783	0.04	0.24

Future research incorporating dynamic stimuli or tasks emphasizing facial expressions could determine whether spatial typicality biases extend to STS-mediated social and emotional processing.

Whole-brain analyses revealed spatial typicality biases in regions extending beyond the visual cortex, particularly within the ventral sensorimotor cortex and the ventromedial prefrontal cortex (vmPFC). The ventral sensorimotor cortex, traditionally associated with motor and somatosensory functions, has been implicated in face processing in prior neuroimaging studies (Taylor et al. 2009; Van de Riet et al. 2009; Rossion et al. 2012; Noad et al. 2024), with some accounts suggesting its role in internally representing perceived facial expressions (Adolphs 2002; Kragel and LaBar 2016; Cao et al. 2018). The vmPFC, a region strongly linked to social cognition, has also been implicated in processing facial identity and making personality inferences (Gobbini et al. 2004; Hiser and Koenigs 2018). These findings are consistent with a growing body of work showing that the recognition of faces depends on an extended network of regions beyond the visual brain (Gobbini and Haxby 2007; Visconti di Oleggio Castello et al. 2017; Kovács 2020; Shoham et al. 2021; Noad et al. 2024).

Our findings suggest that typical spatial location influences the behavioral and neural response to familiar faces. Although average fixation tends to fall near the centre of the face, reliable individual differences in fixation patterns have also been documented (Peterson and Eckstein 2013; Peterson et al. 2016). These individual biases are generally not large enough to substantially alter the overall typical placement of facial features (for instance, the mouth is rarely represented in the upper visual field), but they may nonetheless contribute to variability in the typically experienced location of facial information across visual fields. Future research could therefore usefully examine whether such idiosyncratic fixation patterns predict individual differences in the optimal spatial location for face recognition and the associated neural response.

In conclusion, this study demonstrates that typical spatial configuration plays a fundamental role in familiar face recognition. Familiar faces presented in their typical locations are recognized more accurately and efficiently, with these behavioral effects being mirrored by enhanced neural responses in face-selective regions, particularly the OFA and FFA. Our findings contribute to a growing body of evidence that visual regions associated with recognition are sensitive to statistical regularities in the retinal positioning of familiar objects (DiCarlo and Maunsell 2003; Kravitz et al. 2008, 2010), and that their organization is shaped by these perceptual experiences (Arcaro and Livingstone 2017; Arcaro et al. 2019; Gomez et al. 2019). The presence of spatial typicality biases beyond the visual cortex suggests that spatial organization is not only integral to perceptual processing, but also to higher-order cognitive functions influenced by visual experience, such as social evaluation and affective processing (Groen et al. 2022). These findings underscore the importance of incorporating

spatial factors into models of face recognition and suggest that statistical regularities in natural viewing conditions shape the neural representations of familiar faces across the brain.

Author contributions

Bartholomew Quinn (Conceptualization, Data curation, Formal analysis, Investigation, Methodology, Software, Visualization, Writing—original draft, Writing—review & editing), and Timothy Andrews (Conceptualization, Investigation, Methodology, Supervision, Writing—review & editing).

Supplementary material

Supplementary material is available at *Cerebral Cortex* online.

Funding

The authors received no specific financial support for the research, authorship, and/or publication of this article.

Conflict of interest statement. None declared.

Code availability

Behavioral data, and all analysis code is available on the OSF (https://osf.io/dbufh/).

References

Adolphs R. 2002. Recognizing emotion from facial expressions: psychological and neurological mechanisms. *Behav Cogn Neurosci Rev*. 1:21–62. https://doi.org/10.1177/1534582302001001003.

Ambrus GG, Dotzer M, Schweinberger SR, Kovács G. 2017a. The occipital face area is causally involved in the formation of identity-specific face representations. *Brain Struct Funct*. 222:4271–4282. https://doi.org/10.1007/s00429-017-1467-2.

Ambrus GG, Windel F, Burton AM, Kovács G. 2017b. Causal evidence of the involvement of the right occipital face area in face-identity acquisition. *NeuroImage*. 148:212–218. https://doi.org/10.1016/j.neuroimage.2017.01.043.

Ambrus GG, Amado C, Krohn L, Kovács G. 2019. TMS of the occipital face area modulates cross-domain identity priming. *Brain Struct Funct*. 224:149–157. https://doi.org/10.1007/s00429-018-1768-0.

Andersson JL, Skare S. 2010. Image distortion and its correction in diffusion MRI. In: Jones DK, editor, *Diffusion MRI: theory, methods, and applications*. Oxford University Press, Oxford, pp 285–302.

Arcaro MJ, Livingstone MS. 2017. A hierarchical, retinotopic proto-organization of the primate visual system at birth. *elife*. 6:e26196. https://doi.org/10.7554/eLife.26196.

Arcaro MJ, Schade PF, Livingstone MS. 2019. Universal mechanisms and the development of the face network: what you see is what you get. *Annual review of vision science*. 5:341–372. https://doi.org/10.1146/annurev-vision-091718-014917.

Beckmann CF, Jenkinson M, Smith SM. 2003. General multilevel linear modeling for group analysis in FMRI. *NeuroImage*. 20:1052–1063. https://doi.org/10.1016/S1053-8119(03)00435-X.

Bourne VJ. 2006. The divided visual field paradigm: methodological considerations. *Laterality*. 11:373–393. https://doi.org/10.1080/13576500600633982.

Cao L, Xu J, Yang X, Li X, Liu B. 2018. Abstract representations of emotions perceived from the face, body, and whole-person expressions in the left postcentral gyrus. *Front Hum Neurosci*. 12:419. https://doi.org/10.3389/fnhum.2018.00419.

Carpenter RH. 1988. *Movements of the eyes, 2nd rev*. Pion Limited, London.

Chan AW, Kravitz DJ, Truong S, Arizpe J, Baker CI. 2010. Cortical representations of bodies and faces are strongest in commonly experienced configurations. *Nat Neurosci*. 13:417–418. https://doi.org/10.1038/nn.2502.

Collins JA, Olson IR. 2014. Beyond the FFA: the role of the ventral anterior temporal lobes in face processing. *Neuropsychologia*. 61:65–79. https://doi.org/10.1016/j.neuropsychologia.2014.06.005.

DeBruine L, Jones B. 2017. *Face research lab London set. (Figshare 5047666; version V5) [data set]*. Figshare.

de Haas B, Schwarzkopf DS. 2018. Feature–location effects in the Thatcher illusion. *J Vis*. 18:16–16. https://doi.org/10.1167/18.4.16.

de Haas B et al. 2016. Perception and processing of faces in the human brain is tuned to typical feature locations. *J Neurosci*. 36:9289–9302. https://doi.org/10.1523/JNEUROSCI.4131-14.2016.

de Haas B, Sereno MI, Schwarzkopf DS. 2021. Inferior occipital gyrus is organized along common gradients of spatial and face-part selectivity. *J Neurosci*. 41:5511–5521. https://doi.org/10.1523/JNEUROSCI.2415-20.2021.

DiCarlo JJ, Maunsell JH. 2003. Anterior inferotemporal neurons of monkeys engaged in object recognition can be highly sensitive to object retinal position. *J Neurophysiol*. 89:3264–3278. https://doi.org/10.1152/jn.00358.2002.

Duchaine B, Yovel G. 2015. A revised neural framework for face processing. *Annual review of vision science*. 1:393–416. https://doi.org/10.1146/annurev-vision-082114-035518.

Eick CM, Ambrus GG, Kovács G. 2021. Inhibition of the occipital face area modulates the electrophysiological signals of face familiarity: a combined cTBS-EEG study. *Cortex*. 141:156–167. https://doi.org/10.1016/j.cortex.2021.03.034.

Gobbini MI, Haxby JV. 2007. Neural systems for recognition of familiar faces. *Neuropsychologia*. 45:32–41. https://doi.org/10.1016/j.neuropsychologia.2006.04.015.

Gobbini MI, Leibenluft E, Santiago N, Haxby JV. 2004. Social and emotional attachment in the neural representation of faces. *NeuroImage*. 22:1628–1635. https://doi.org/10.1016/j.neuroimage.2004.03.049.

Golarai G, Liberman A, Grill-Spector K. 2015. Experience shapes the development of neural substrates of face processing in human ventral temporal cortex. *Cereb Cortex*. 27:1229–1244. https://doi.org/10.1093/cercor/bhv314.

Gomez J, Barnett M, Grill-Spector K. 2019. Extensive childhood experience with Pokémon suggests eccentricity drives organization of visual cortex. *Nat Hum Behav*. 3:611–624. https://doi.org/10.1038/s41562-019-0592-8.

Greve DN, Fischl B. 2009. Accurate and robust brain image alignment using boundary-based registration. *NeuroImage*. 48:63–72. https://doi.org/10.1016/j.neuroimage.2009.06.060.

Groen II, Dekker TM, Knapen T, Silson EH. 2022. Visuospatial coding as ubiquitous scaffolding for human cognition. *Trends Cogn Sci*. 26:81–96. https://doi.org/10.1016/j.tics.2021.10.011.

Harris RJ, Young AW, Andrews TJ. 2014. Brain regions involved in processing facial identity and expression are differentially selective for surface and edge information. *NeuroImage*. 97:217–223. https://doi.org/10.1016/j.neuroimage.2014.04.032.

Harrison MT, Strother L. 2020. Does right hemisphere superiority sufficiently explain the left visual field advantage in face recognition? *Atten Percept Psychophys*. 82:1205–1220. https://doi.org/10.3758/s13414-019-01896-0.

Hasson U, Levy I, Behrmann M, Hendler T, Malach R. 2002. Eccentricity bias as an organizing principle for human high-order object areas. *Neuron*. 34:479–490. https://doi.org/10.1016/S0896-6273(02)00662-1.

Haxby JV, Hoffman EA, Gobbini MI. 2000. The distributed human neural system for face perception. *Trends Cogn Sci*. 4:223–233. https://doi.org/10.1016/S1364-6613(00)01482-0.

Henriksson L, Mur M, Kriegeskorte N. 2015. Faciotopy – a face-feature map with face-like topology in the human occipital face area. *Cortex*. 72:156–167. https://doi.org/10.1016/j.cortex.2015.06.030.

Hiser J, Koenigs M. 2018. The multifaceted role of the ventromedial prefrontal cortex in emotion, decision making, social cognition, and psychopathology. *Biol Psychiatry*. 83:638–647. https://doi.org/10.1016/j.biopsych.2017.10.030.

Hsiao JHW, Cottrell G. 2008. Two fixations suffice in face recognition. *Psychol Sci*. 19:998–1006. https://doi.org/10.1111/j.1467-9280.2008.02191.x.

Hsiao JHW, Shieh DX, Cottrell GW. 2008. Convergence of the visual field split: hemispheric modeling of face and object recognition. *J Cogn Neurosci*. 20:2298–2307. https://doi.org/10.1162/jocn.2008.20162.

Iordan MC, Greene MR, Beck DM, Fei-Fei L. 2016. Typicality sharpens category representations in object-selective cortex. *NeuroImage*. 134:170–179. https://doi.org/10.1016/j.neuroimage.2016.04.012.

Jenkinson M, Bannister P, Brady M, Smith S. 2002. Improved optimization for the robust and accurate linear registration and motion correction of brain images. *NeuroImage*. 17:825–841. https://doi.org/10.1006/nimg.2002.1132.

Jonas J et al. 2012. Focal electrical intracerebral stimulation of a face-sensitive area causes transient prosopagnosia. *Neuroscience*. 222:281–288. https://doi.org/10.1016/j.neuroscience.2012.07.021.

Kanwisher N. 2010. Functional specificity in the human brain: a window into the functional architecture of the mind. *Proc Natl Acad Sci*. 107:11163–11170. https://doi.org/10.1073/pnas.1005062107.

Kovács G. 2020. Getting to Know Someone: Familiarity, Person Recognition, and Identification in the Human Brain. *Journal of Cognitive Neuroscience*. 32:2205–2225. https://doi.org/10.1162/jocn_a_01627.

Kragel PA, LaBar KS. 2016. Decoding the nature of emotion in the brain. *Trends Cogn Sci*. 20:444–455. https://doi.org/10.1016/j.tics.2016.03.011.

Kravitz DJ, Vinson LD, Baker CI. 2008. How position dependent is visual object recognition? *Trends Cogn Sci*. 12:114–122. https://doi.org/10.1016/j.tics.2007.12.006.

Kravitz DJ, Kriegeskorte N, Baker CI. 2010. High-level visual object representations are constrained by position. *Cereb Cortex*. 20:2916–2925. https://doi.org/10.1093/cercor/bhq042.

Langner O et al. 2010. Presentation and validation of the Radboud faces database. *Cognit Emot*. 24:1377–1388. https://doi.org/10.1080/02699930903485076.

Levy I, Hasson U, Avidan G, Hendler T, Malach R. 2001. Center–periphery organization of human object areas. *Nat Neurosci*. 4:533–539. https://doi.org/10.1038/87490.

Ma DS, Kantner J, Wittenbrink B. 2021. Chicago face database: multiracial expansion. *Behav Res Methods*. 53:1289–1300. https://doi.org/10.3758/s13428-020-01482-5.

Morsi AY et al. 2024. Common patterns of spatial selectivity in early visual cortex and face-selective brain regions. *bioRxiv*, 2024-05. https://doi.org/10.1101/2024.05.14.594166.

Noad KN, Watson DM, Andrews TJ. 2024. Familiarity enhances functional connectivity between visual and nonvisual regions of the brain during natural viewing. *Cereb Cortex*. 34:bhae285. https://doi.org/10.1093/cercor/bhae285.

Oldfield RC. 1971. The assessment and analysis of handedness: The Edinburgh inventory. *Neuropsychologia*. 9:97–113. https://doi.org/10.1016/0028-3932(71)90067-4.

Peterson MF, Eckstein MP. 2012. Looking just below the eyes is optimal across face recognition tasks. *Proc Natl Acad Sci*. 109:E3314–E3323. https://doi.org/10.1073/pnas.1214269109.

Peterson MF, Eckstein MP. 2013. Individual differences in eye movements during face identification reflect observer-specific optimal points of fixation. *Psychol Sci*. 24:1216–1225. https://doi.org/10.1177/0956797612471684.

Peterson MF, Lin J, Zaun I, Kanwisher N. 2016. Individual differences in face-looking behavior generalize from the lab to the world. *J Vis*. 16:12–12. https://doi.org/10.1167/16.7.12.

Pitcher D, Ungerleider LG. 2021. Evidence for a third visual pathway specialized for social perception. *Trends Cogn Sci*. 25:100–110. https://doi.org/10.1016/j.tics.2020.11.006.

Rossion B, Hanseeuw B, Dricot L. 2012. Defining face perception areas in the human brain: a large-scale factorial fMRI face localizer analysis. *Brain Cogn*. 79:138–157. https://doi.org/10.1016/j.bandc.2012.01.001.

Shoham A, Kliger L, Yovel G. 2021. Learning faces as concepts improves face recognition by engaging the social brain network. *Social Cognitive and Affective Neuroscience*. 17:290–299. https://doi.org/10.1093/scan/nsab096.

Silson EH, Groen II, Kravitz DJ, Baker CI. 2016. Evaluating the correspondence between face-, scene-, and object-selectivity and retinotopic organization within lateral occipitotemporal cortex. *J Vis*. 16:14–14. https://doi.org/10.1167/16.6.14.

Silson EH, Groen II, Baker CI. 2022. Direct comparison of contralateral bias and face/scene selectivity in human occipitotemporal cortex. *Brain Struct Funct*. 227:1405–1421. https://doi.org/10.1007/s00429-021-02411-8.

Smith SM. 2002. Fast robust automated brain extraction. *Hum Brain Mapp*. 17:143–155. https://doi.org/10.1002/hbm.10062.

Taylor MJ et al. 2009. Neural correlates of personally familiar faces: parents, partner and own faces. *Hum Brain Mapp*. 30:2008–2020. https://doi.org/10.1002/hbm.20646.

Valentine T. 1988. Upside-down faces: a review of the effect of inversion upon face recognition. *Br J Psychol*. 79:471–491. https://doi.org/10.1111/j.2044-8295.1988.tb02747.x.

Van de Riet WA, Grèzes J, de Gelder B. 2009. Specific and common brain regions involved in the perception of faces and bodies and the representation of their emotional expressions. *Soc Neurosci*. 4:101–120. https://doi.org/10.1080/17470910701865367.

van den Hurk J, Pegado F, Martens F, de Beeck HPO. 2015. The search for the face of the visual homunculus. *Trends Cogn Sci*. 19:638–641. https://doi.org/10.1016/j.tics.2015.09.007.

Vieira TF, Bottino A, Laurentini A, De Simone M. 2014. Detecting siblings in image pairs. *Vis Comput*. 30:1333–1345. https://doi.org/10.1007/s00371-013-0884-3.

Visconti di Oleggio Castello M, Halchenko YO, Guntupalli JS, Gors JD, Gobbini MI. 2017. The neural representation of personally familiar and unfamiliar faces in the distributed system for face perception. *Scientific Reports*. 7. https://doi.org/10.1038/s41598-017-12559-1

Walker-Smith GJ, Gale AG, Findlay JM. 2013. Eye movement strategies involved in face perception. *Perception*. 42:1120–1133. https://doi.org/10.1068/p060313n.

Wandell BA, Dumoulin SO, Brewer AA. 2007. Visual field maps in human cortex. *Neuron*. 56:366–383. https://doi.org/10.1016/j.neuron.2007.10.012.

Wang L, Mruczek RE, Arcaro MJ, Kastner S. 2015. Probabilistic maps of visual topography in human cortex. *Cereb Cortex*. 25:3911–3931. https://doi.org/10.1093/cercor/bhu277.

Woolrich M. 2008. Robust group analysis using outlier inference. *NeuroImage*. 41:286–301. https://doi.org/10.1016/j.neuroimage.2008.02.042.

Woolrich MW, Behrens TE, Beckmann CF, Jenkinson M, Smith SM. 2004. Multilevel linear modelling for FMRI group analysis using Bayesian inference. *NeuroImage*. 21:1732–1747. https://doi.org/10.1016/j.neuroimage.2003.12.023.

Xiao J, Hays J, Ehinger KA, Oliva A, Torralba A. 2010. Sun database: Large-scale scene recognition from abbey to zoo. In: 2010 *IEEE computer society conference on computer vision and pattern recognition*. [dataset]. IEEE, pp 3485–3492.

Young AW. 1982. Methodological theoretical bases. In: Beaumont JG, editor, *Divided visual field studies of cerebral organisation*. Academic Press, London, pp. 11–27.

Cerebral Cortex, 2025, **35**, bhaf328
https://doi.org/10.1093/cercor/bhaf328
Original Article